CONVERTING A STEERING KNUCKLE INTO A 6-DOF FORCE TRANSDUCER

M.C. Witter, S.M. Dumbacher, and D.L. Brown

Structural Dynamics Research Laboratory
University of Cincinnati, P.O. Box 210072
Cincinnati, Ohio 45221-0072 USA

ABSTRACT

An array of strain gages is used to convert the steering knuckle of a Mercury Sable into a six degree-of-freedom (6-DOF) force transducer. The three translation forces and three moments entering the steering knuckle from the wheel are estimated using operating strain gage responses and the inverse FRF method. The strain gage array is calibrated using a 6-DOF load cell. The load cell is calibrated using a rigid body calibration mass with known inertia properties. The motion of the calibration mass is measured with perimeter reference accelerometers.

NOMENCLATURE

$[.]^{+}$ = pseudo-inverse of [.]
$[.]^{H}$ = hermitian of [.]
$[\psi]$ = rigid body transformation matrix
$\underline{q}$ = vector of rigid body translations; vector of reference accelerometer responses
$\underline{F}_p$ = vector of 6 inputs at point p
$[G_{F_pF_p}]$ = auto spectral matrix of 6 input forces at point p
$[G_{XLCF_p}$ = cross spectral matrix between 8 load cell outputs and 6 input forces at point p
$[G_{XSGF_p}]$ = cross spectral matrix between 18 strain gage outputs and 6 input forces at point p
$[H_{LCcal}]$ = FRF matrix between load cell and point p; load cell calibration matrix
$[H_{SGcal}]$ = FRF matrix between strain gage array and point p; strain gage array calibration matrix
[IM] = inertia matrix
$\underline{K}_p$ = vector of rigid body modal participation factors; vector of 6 accelerations at point p
Navg = number of averages in FRF estimation
Nref = number of perimeter reference accelerometers
$\underline{X}_{LC}$ = vector of load cell responses
$\underline{X}_{SG}$ = vector of strain gage responses
[W] = weighting matrix applied to exclude references
DOF = degree-of-freedom
FRF = frequency response function

1. INTRODUCTION

The goal of this project was to estimate the operating wheel translation force and moment inputs to a Mercury Sable steering knuckle, without making modifications to the existing steering knuckle. The wheel assembly bolts to the steering knuckle at three locations. All forces and moments entering the steering knuckle from the wheel assembly must pass through these three bolt locations. The brake pad also connects to the steering knuckle, but was removed for the testing.

A method which does not require modifications to the steering knuckle is to calibrate an array of strain gages placed on the steering knuckle to the 6 force and moment inputs. The strain gages are ICP piezo-electric transducers. Previous noise path analysis testing [1,2] indicated that the ICP strain gages produce accurate force estimates down to very low frequencies (3-6 Hz), and are good transducers for noise path analysis applications.

The strain gage array is calibrated prior to operating conditions using impact testing and the inverse FRF method. A 6-dof load cell is used in the array calibration procedure to provide an estimate of the 6 force and moment inputs at a point on the plate bolted to the steering knuckle. Once the array is calibrated, the load cell is removed from the system. The wheel assembly may then be re-attached to the vehicle and operating data acquired.

The 6-DOF load cell is calibrated using impact testing with a rigid body calibration mass of known inertia properties [3-6]. The motion of the calibration mass is measured with perimeter reference accelerometers. The forces generated due to the calibration mass motion are estimated using F=ma. Current research applications of the 6-DOF load cell include rigid body inertia properties testing and noise path analysis testing.

This method of array calibration does not account for forces entering the steering knuckle through other points. The body side of the steering knuckle is attached to the strut, the tie rod, and the control arm. To convert the steering knuckle into a complete 6-DOF force transducer, the 6 forces and moments at each attachment point should be accounted for. This would result in a strain gage array calibration matrix that is

valid for all operating configurations of the vehicle. However, this would require at least six response measurements for each attachment point and a calibration using the 6-DOF load cell at each attachment point. As a result, only the wheel-side attachment point of the steering knuckle was taken into account. This means that the strain gage array calibration may change if the steering knuckle boundary conditions change. To investigate this, operating data was acquired with the vehicle in four different configurations. The first vehicle configuration is a baseline configuration with the vehicle suspended at level height with a 0° steering angle. The other three configurations simulate the conditions of driving over a bump and turning the vehicle. The baseline configuration calibration matrix was used to process each operating data set.

2. THEORY

The calibration of the strain gage array relates the outputs of the strain gages to the six operating inputs to the steering knuckle. The six inputs, three translation forces and three moments, are computed at a single point p. Point p is located at the center of the load cell base, where the load cell is attached to the wheel side of the steering knuckle.

A 6-DOF load cell is used to calibrate the strain gage array prior to operating conditions. The load cell with the impact mass attached is calibrated, independent of the steering knuckle, to relate the outputs of the load cell to the six inputs at point p.

2.1 Calibration of 6-DOF Load Cell

The relationship between the outputs of the load cell, $\underline{X}_{LC}$, and the six input forces at a point p, $\underline{F}_p$, can be expressed in the frequency domain as

$$\underline{X}_{LC} = [H_{LCcal}]\underline{F}_p \tag{1}$$

where $[H_{LCcal}]$ is the frequency response function (FRF) matrix, or the calibration matrix of the load cell. $\underline{F}_p$ is needed to compute the calibration matrix.

$\underline{F}_p$ is obtained with perimeter reference accelerometers placed on a rigid body calibration mass with known inertia properties. The load cell is attached to the calibration mass. An impact mass is attached to the other side of the load cell. The entire calibration fixture is suspended with soft cables to simulate a free-free boundary condition. Impacts are applied to the impact mass. All forces and moments causing motion of the calibration mass must pass through the load cell. By using the translation measurements from the perimeter reference accelerometers, the three translation and three rotation accelerations at any point p on the rigid body can be computed.

The translation $\underline{q}$ of any point i on a rigid body can be described as a superposition of the rigid body modes,

$$\underline{q}_i = [\Psi_i]\underline{K}_p \tag{2}$$

where $[\psi_i]$ is the rigid body transformation matrix for point i and $\underline{K}_p$ is the vector of six modal participation factors. If the rigid body modes are scaled to unity displacement at point p, $\underline{K}_p$ is equal to the translation and rotation accelerations at point p.

$$\begin{Bmatrix} \ddot{x}_i \\ \ddot{y}_i \\ \ddot{z}_i \end{Bmatrix} = \begin{bmatrix} 1 & 0 & 0 & 0 & z_i & -y_i \\ 0 & 1 & 0 & -z_i & 0 & x_i \\ 0 & 0 & 1 & y_i & -x_i & 0 \end{bmatrix} \begin{Bmatrix} \ddot{x}_p \\ \ddot{y}_p \\ \ddot{z}_p \\ \ddot{\theta}_{x_p} \\ \ddot{\theta}_{y_p} \\ \ddot{\theta}_{z_p} \end{Bmatrix} \tag{3}$$

where x_i, y_i, and z_i indicate the position of point i in a coordinate system with origin point p. To solve for the six accelerations at point p, at least six independent pieces of information are needed, or two triaxial measurement points. By adding additional measurement points, the system can be over-determined. Equation (3) is expanded as

$$\underline{q} = \begin{Bmatrix} \underline{q}_1 \\ \underline{q}_2 \\ \vdots \\ \underline{q}_{Nref} \end{Bmatrix} = \begin{bmatrix} [\Psi_1] \\ [\Psi_2] \\ \vdots \\ [\Psi_{Nref}] \end{bmatrix} \underline{K}_p = [\Psi]\underline{K}_p \tag{4}$$

where *Nref* is the number of perimeter reference triaxial accelerometers. A diagonal weighting matrix can be used to allow for selection of references to be included in the solution. Pre-multiplying both sides of equation (4) by the weighting matrix [W] and solving for $\underline{K}_p$ using a least-squares pseudo-inverse procedure results in

$$\underline{K}_p = ([W][\Psi])^{+}[W]\underline{q} \quad . \tag{5}$$

Equation (5) estimates the translation and rotation accelerations at a point p on the rigid body, based on the translation measurements of the perimeter reference accelerometers. The resulting input forces and moments at point p are estimated from the motion of the rigid body using F=ma. Substituting the rigid body inertia property matrix of the calibration mass calculated about point p results in

$$\begin{Bmatrix} F_x \\ F_y \\ F_z \\ M_x \\ M_y \\ M_z \end{Bmatrix}_p = \begin{bmatrix} m & 0 & 0 & 0 & mz_{cg} & -my_{cg} \\ 0 & m & 0 & -mz_{cg} & 0 & mx_{cg} \\ 0 & 0 & m & my_{cg} & -mx_{cg} & 0 \\ 1 & 0 & 0 & I_{xx} & -I_{xy} & -I_{xz} \\ 0 & 1 & 0 & -I_{yx} & I_{yy} & -I_{yz} \\ 0 & 0 & 1 & -I_{zx} & -I_{zy} & I_{zz} \end{bmatrix} \begin{Bmatrix} \ddot{x} \\ \ddot{y} \\ \ddot{z} \\ \ddot{\theta}_x \\ \ddot{\theta}_y \\ \ddot{\theta}_z \end{Bmatrix}_p \quad (6)$$

where F_x, F_y and F_z are the three translation forces at point p, and M_x, M_y, and M_z are the three moments at point p. Substituting $\underline{K}_p$ from equation (5) into equation (6) results in

$$\underline{F}_p = [IM]\underline{K}_p = [IM]([W][\Psi])^+[W]\underline{q} \quad (7)$$

where $\underline{F}_p$ is the vector of six inputs at point p and [IM] is the inertia matrix expressed in equation (6).

Equation (7) relates the six inputs at point p to the *Nref* triaxial translation measurements from the perimeter reference accelerometers. The calibration of the load cell was given in equation (1) as

$$\underline{X}_{LC} = [H_{LCcal}]\underline{F}_p \quad . \quad (1)$$

The calibration matrix $[H_{LCcal}]$ is calculated using an H_1 FRF estimate

$$[H_{LCcal}] = [G_{X_{LC}F_P}][G_{F_pF_p}]^{-1} \quad (8)$$

where $[G_{XLCFp}]$ is the cross spectral matrix between the load cell outputs and the six input forces at point p and $[G_{FpFp}]$ is the auto spectral matrix of the six input forces at point p. Averaging in the FRF estimate is done by impacting at different points on the impact mass to excite all degrees of freedom of the calibration mass. The responses of the load cell and the perimeter reference accelerometers for each impact then form a column for each response matrix, as shown in equations (9) and (10). The auto and cross spectral matrices are computed as

$$[G_{X_{LC}F_P}] = \left[\{X_{LC}\}_1 \ \{X_{LC}\}_2 \cdots \{X_{LC}\}_{Navg}\right] * \left[\{F_p\}_1 \ \{F_p\}_2 \cdots \{F_p\}_{Navg}\right]^H \quad (9)$$

$$[G_{F_pF_p}] = \left[\{F_p\}_1 \{F_p\}_2 \cdots \{F_p\}_{Navg}\right] * \left[\{F_p\}_1 \{F_p\}_2 \cdots \{F_p\}_{Navg}\right]^H \quad (10)$$

where *Navg* is the number of averages used in the impact test.

2.2 Calibration of Strain Gage Array

Once the 6-DOF load cell is calibrated, the load cell and impact mass are attached to the instrumented steering knuckle located on the vehicle. The array is calibrated by impacting on the impact mass at various locations and measuring the responses of the strain gages and the load cell. The array calibration procedure is similar to the load cell calibration procedure, except the six input forces are now measured with the load cell.

The relationship between the strain gage outputs, $\underline{X}_{SG}$, and the six input forces at a point p, $\underline{F}_p$, can be expressed in the frequency domain as

$$\underline{X}_{SG} = [H_{SGcal}]\underline{F}_p \quad (11)$$

where $[H_{SGcal}]$ is the FRF matrix, or the calibration matrix of the strain gage array.

The force $\underline{F}_p$ is obtained from equation (1) by taking the pseudo-inverse of the 6-DOF load cell calibration matrix

$$\underline{F}_p = [H_{LCcal}]^+\underline{X}_{LC} \quad . \quad (12)$$

The strain gage array calibration matrix $[H_{SGcal}]$ is calculated using an H_1 FRF estimate

$$[H_{SGcal}] = [G_{X_{SG}F_P}][G_{F_pF_p}]^{-1} \quad (13)$$

where $[G_{XSGFp}]$ is the cross spectral matrix between the strain gage outputs and the six input forces at point p, and $[G_{FpFp}]$ is the auto spectral matrix of the six input forces at point p. Averaging in the FRF estimate is done by impacting at different points on the impact mass, similar to the procedure used in the load cell calibration. The cross spectral matrix is computed as

$$[G_{X_{SG}F_P}] = \left[\{X_{SG}\}_1 \ \{X_{SG}\}_2 \cdots \{X_{SG}\}_{Navg}\right] * \left[\{F_p\}_1 \ \{F_p\}_2 \cdots \{F_p\}_{Navg}\right]^H \quad (14)$$

where each column of the response matrices corresponds to a single impact. The auto spectral matrix $[G_{FpFp}]$ is computed using equation (10), with equation (12) substituted for $\underline{F}_p$.

2.3 Estimation of Operating Inputs

Once the strain gage array has been calibrated, the 6-DOF load cell is no longer needed. The wheel can be replaced and operating strain gage data acquired. The estimate of the operating input force $\underline{F}_p$ is obtained from equation (11) using the pseudo-inverse of the strain gage array calibration matrix

$$\underline{F}_p = [H_{SGcal}]^+ \underline{X}_{SG} \quad . \tag{15}$$

3. 6-DOF LOAD CELL CALIBRATION

The 6-DOF load cell, shown in figure 1, has two pairs of shear crystals and two pairs of compression crystals. The plating on the crystals is segmented to collect charge from each half independently, resulting in eight outputs.

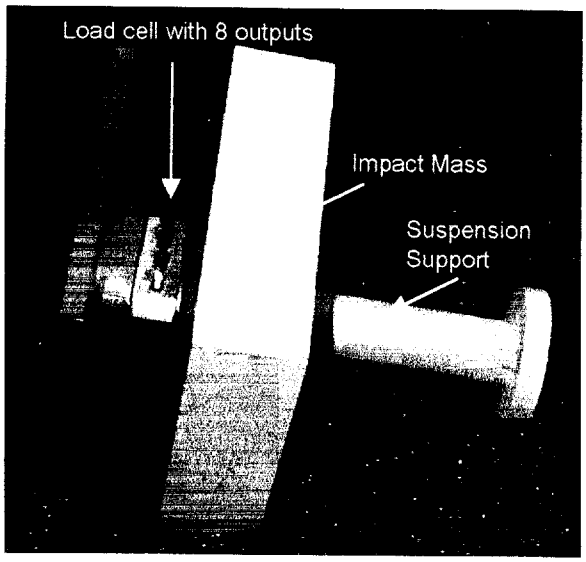

Figure 1: *6-DOF load cell with impact mass.*

To calibrate the load cell, an impact mass was bolted to one side of the load cell and a rigid body calibration mass bolted to the other side of the load cell, as shown in figure 2. 8 triaxial accelerometers were placed on the calibration mass as perimeter references. The calibration fixture was suspended with soft supports to simulate a free-free boundary condition.

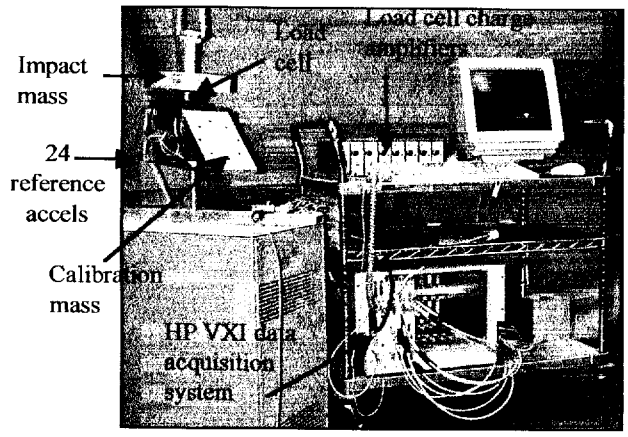

Figure 2: *6-DOF load cell calibration setup.*

25 impacts were applied to the impact mass to excite as many degrees of freedom of the calibration mass as possible. The accelerometer and load cell responses were acquired for a frequency range of 0-1024 Hz, with each impact set forming a column in the response matrices for the FRF estimate averaging, as shown in equations (9) and (10).

In order to calibrate the load cell accurately, a complete set of forces must be generated in the load cell. These forces are proportional to the inertia matrix of the calibration fixture. By modifying the configuration of the calibration fixture, a different set of forces is generated in the load cell. Six configurations of the calibration fixture were selected, as shown in figure 3. Each configuration results in a different inertia matrix and CG location with respect to the base of the load cell. As a result, different forces are excited for each of the six configurations. Testing six configurations results in a more complete force set than testing only one configuration.

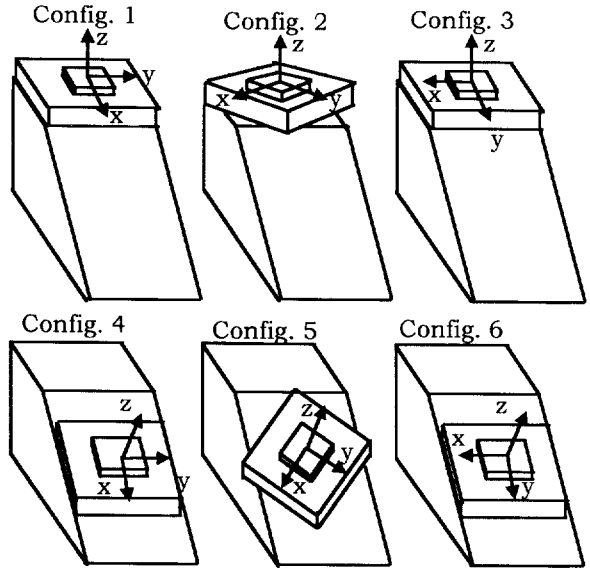

Figure 3: *Six configurations of load cell calibration impact tests, with load cell coordinate axes.*

The 6 inputs at point p were computed using the 8 perimeter reference triaxial accelerometers. The load cell calibration matrix was calculated using an H_1 FRF estimate, as described in section 2.1.

The load cell calibration matrix was computed for each configuration separately. The calibration curves of each configuration were then averaged for a load cell calibration matrix as a function of frequency.

Sample load cell calibration curves as a function of frequency are presented in figure 4 for the x-direction translation force and the z-direction moment. The curves are relatively flat across the frequency range, with some error near 600 Hz. At this frequency, a nonlinear torsion mode of the calibration fixture exists. The mean values of the calibration curves between 100 Hz and 400 Hz were taken for a frequency independent load cell calibration matrix of size 8x6. The pseudo-

inverse of the 8x6 matrix was computed and stored for use in the strain gage array calibration.

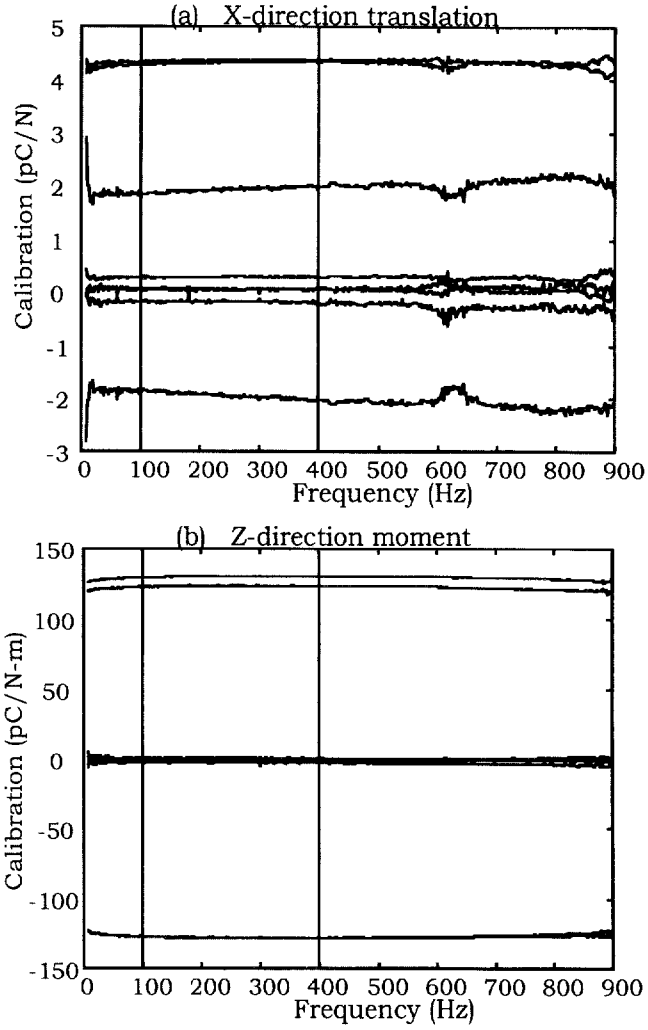

Figure 4: *Sample load cell calibration curves.*

The multiple coherence between the 8 load cell outputs and the 6 inputs at point p is shown in figure 5 for a configuration exhibiting the lowest coherence values. The coherence is approximately 1 across the frequency range of interest for 7 of the 8 load cell outputs. For one load cell output, there is a slight dip in coherence near the nonlinear torsion mode of the calibration fixture.

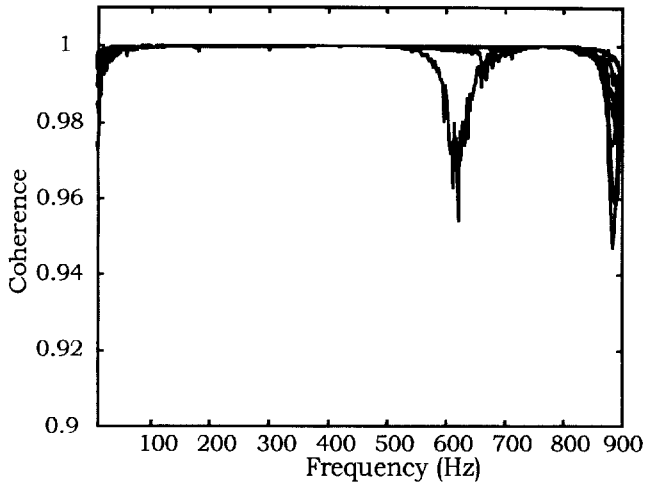

Figure 5: *Multiple coherence for configuration 4.*

4. STRAIN GAGE ARRAY CALIBRATION

The passenger side steering knuckle of a Mercury Sable was instrumented with 18 ICP strain gages, as shown in figure 6. Flats were ground on the steering knuckle to ensure the strain gages made complete contact with the surface of the steering knuckle. The locations of the strain gages were selected to be non-intrusive for an operating road test. The exact locations and orientations were otherwise selected somewhat randomly. Ideally, a finite element model of the steering knuckle would be built and the strain gages placed in areas of high strain. With 18 strain gages and 6 inputs to estimate, the system is over-determined by a factor of 3.

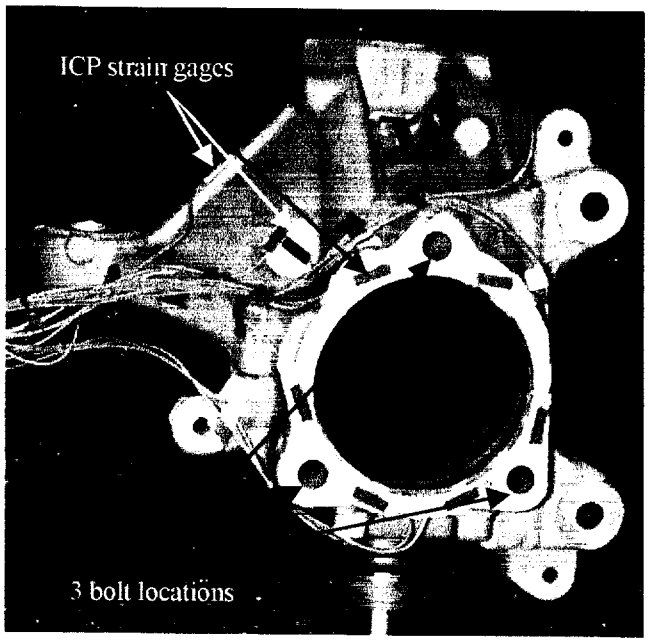

Figure 6: *Steering knuckle instrumented with 18 ICP strain gages.*

The steering knuckle has 3 bolt locations where inputs from the wheel can enter, as shown in figure 6. A small triangular plate was constructed and bolted to the steering knuckle at these 3 locations. The instrumented steering knuckle and plate were re-attached to the vehicle. The calibrated load cell and impact mass were then bolted to the plate. The vehicle was suspended to level height with a strap, as shown in figure 7.

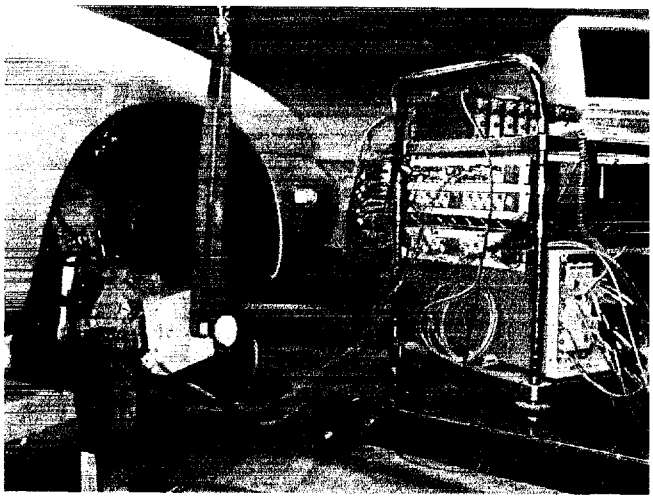

Figure 7: *Instrumented steering knuckle and impact mass attached to Mercury Sable.*

50 impacts were applied to the impact mass for averaging in the FRF estimate procedure, as shown in figure 8. The strain gage and load cell responses were acquired for a frequency range of 0-1024 Hz and a 1 Hz frequency resolution, with each impact set forming a column in the response matrices for the FRF estimate averaging, as shown in equations (10) and (14).

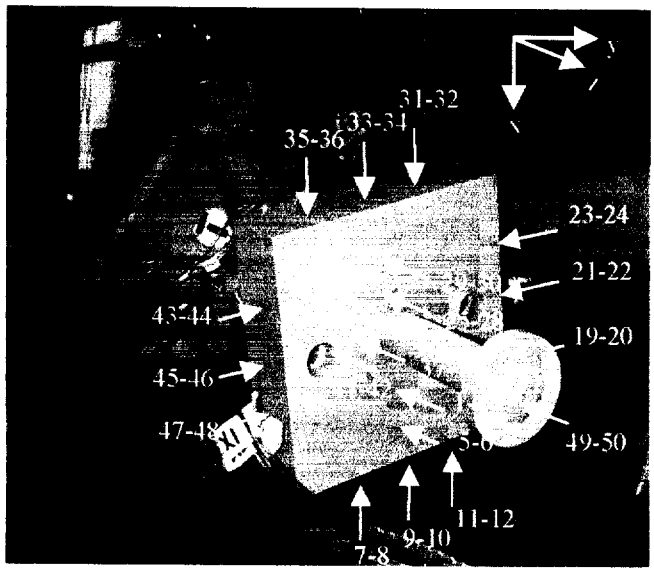

Figure 8: *50 impact locations for calibration of strain gage array.*

An impact hammer was used for the impact testing. The modal punch was used to impact at locations which were difficult to access, as shown in figure 9.

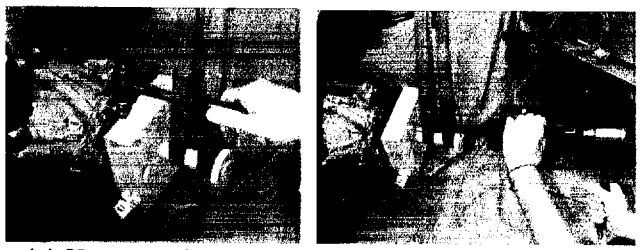

(a) Hammer impact (b) Modal punch impact

Figure 9: *Impacting mass with (a) hammer, and (b) modal punch.*

The 6 inputs at point p were computed using the calibrated load cell. The strain gage array calibration matrix was calculated using an H_1 FRF estimate, as described in section 2.2. The size of the calibration matrix is 18x6 for each spectral line.

Figure 10 shows sample strain gage array calibration curves as a function of frequency. The curves are not flat, due to the modes of the system. However, since the inverse FRF method is used, the linear modes of the system should be calibrated out in the final results. Note in figure 10 that the sensitivities of 5 of the strain gages are approximately 30-40 dB below those of the other 13 strain gages. This is due either to the nominal sensitivity of the strain gages, or to the placement of the strain gages. Since the system is

over-determined by 12 strain gages, it is possible to remove the signals of the 5 strain gages from the estimation procedure. In this analysis, no attempt to remove strain gages or determine optimal placement was done.

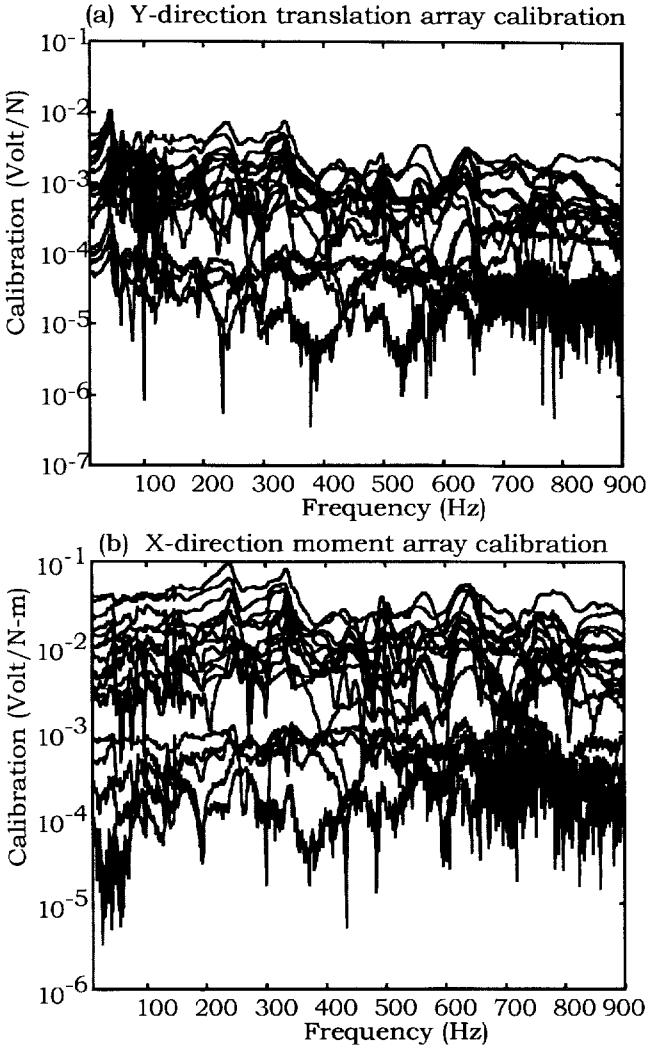

Figure 10: *Sample strain gage array calibration curves for baseline case.*

The multiple coherence between the 18 strain gage outputs and the 6 inputs at point p is shown in figure 11. The coherence for 13 of the strain gages is above .9 across of the frequency range of interest, except near 300 Hz. A nonlinear mode of the system probably occurs at this frequency. The 5 strain gages that had 30-40 dB lower sensitivities exhibit lower coherence across the frequency range, especially above 600 Hz.

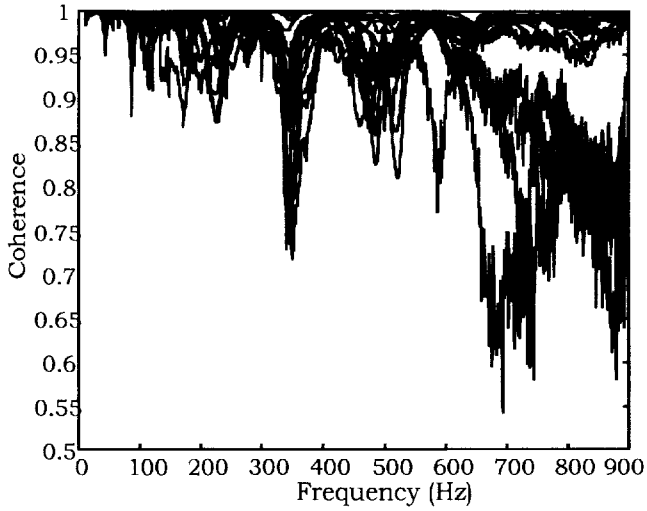

Figure 11: *Multiple coherence for baseline case.*

5. ESTIMATION OF OPERATING INPUT FORCES

For a road operating test, the load cell and impact mass would be removed and the wheel re-attached to the vehicle. Before the array calibration method is tested with road operating data, it must first be verified with controlled laboratory operating data. To verify the accuracy of the analysis procedure, the load cell remained in place with the impact mass. The strain gage operating input estimates were then compared with the load cell operating input estimates.

Operating data was acquired by impacting at various points on the impact mass and measuring the load cell and strain gage responses. This was done for 4 different configurations of the vehicle. The first configuration was the vehicle suspended at level height with a 0° steering angle. This is the baseline configuration of the vehicle, used for the strain gage array calibration. The second configuration was the vehicle suspended at a height of 5" above level with a 0° steering angle. This configuration represents an extreme case of suspension compression. The third and fourth configurations were at the level height with a 25° steering angle to the right and to the left, respectively. These configurations represent the extreme cases of turning the vehicle. Each of the operating data sets was processed using the baseline configuration strain gage array calibration matrix.

5.1 Baseline Configuration Operating Results

Figure 12 shows sample operating input estimates for an impact in the lateral z-direction of the vehicle, using the strain gage array and using the load cell. The results shown in figure 12 are typical results. The estimates from the strain gage array compare very well with the results from the load cell.

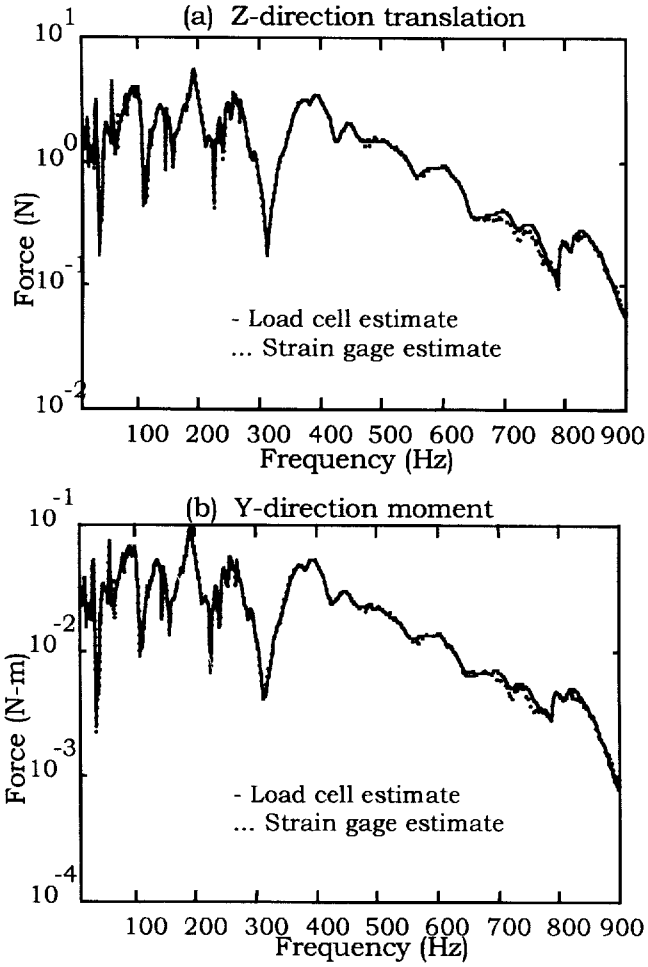

Figure 12: *Typical "best results" operating force input estimates using load cell and strain gage array.*

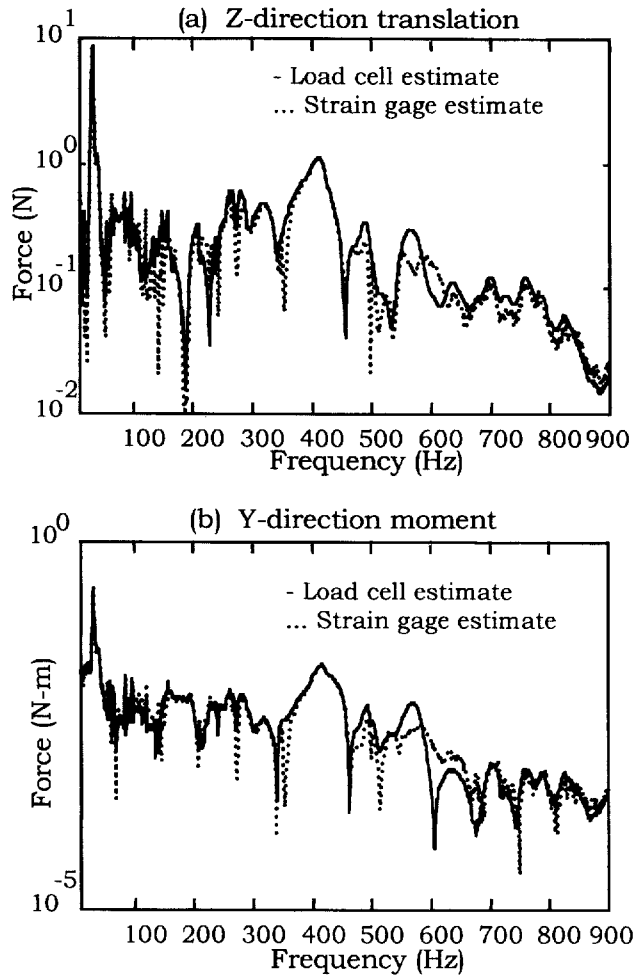

Figure 13: *Typical "worst results" operating force input estimates using load cell and strain gage array.*

Figure 13 shows sample operating input estimates for an impact in the y-direction, using the strain gage array and using the load cell. The results shown in figure 13 are typical worst results of the baseline configuration. Impacting in the y-direction, or the fore-aft direction of the vehicle, excites a very lightly damped mode near 20 Hz. The estimates from the strain gage array compare fairly well with the results from the load cell, with some discrepancies in the 500-600 Hz range.

5.2 Configuration 2 (5" Above Level Height) Operating Results

Figure 14 shows sample operating input estimates for an impact in the vertical x-direction of the vehicle, using the strain gage array and using the load cell. The results shown in figure 14 are typical results for this configuration. The estimates from the strain gage array compare fairly well with the results from the load cell, especially below 300 Hz. This indicates that the calibration matrix does not vary significantly as a function of height.

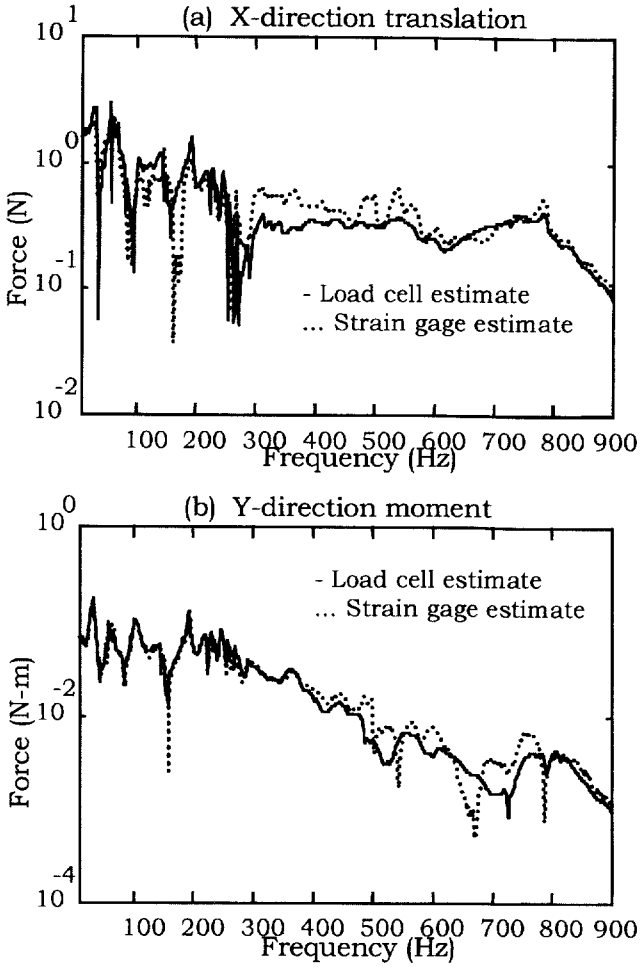

Figure 14: *Sample operating force estimates using baseline calibration matrix and height 2 operating data.*

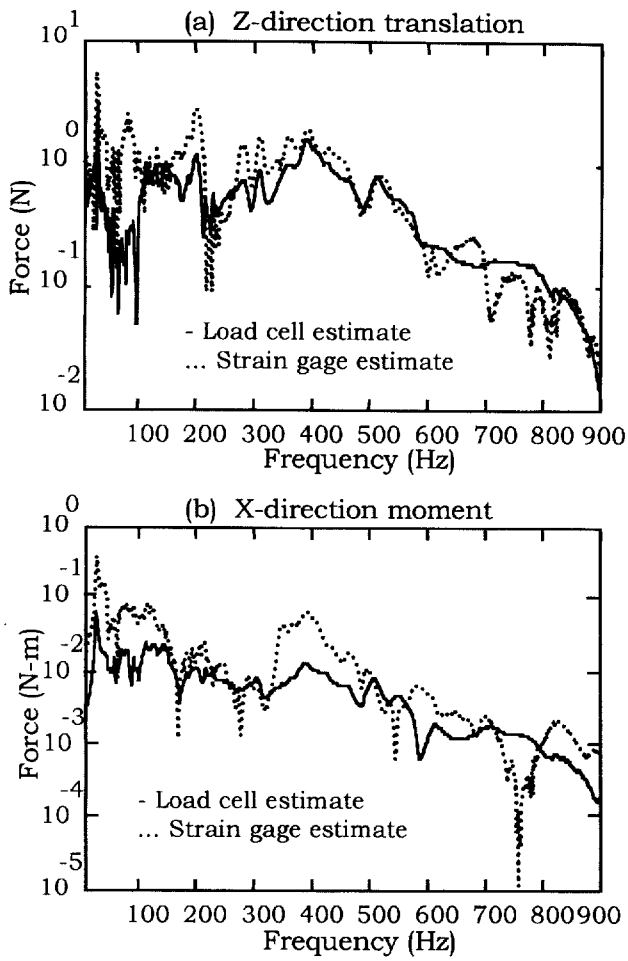

Figure 15: *Sample operating force estimates using baseline calibration matrix and steering angle 25° to right operating data.*

5.3 Configuration 3 (Steering Angle 25° to Right) Operating Results

Figure 15 shows sample operating input estimates for an impact in the lateral z-direction of the vehicle, using the strain gage array and using the load cell. The results shown in figure 15 are typical results for this configuration. The estimates from the strain gage array have the same general shape as the results from the load cell, but have a 10-20 dB difference in both the translation force and moment estimates at many frequencies. This indicates that the calibration matrix varies significantly with a large steering angle.

5.4 Configuration 4 (Steering Angle 25° to Left) Operating Results

Figure 16 shows sample operating input estimates for an impact in the lateral z-direction of the vehicle, using the strain gage array and using the load cell. The results shown in figure 16 are typical results for this configuration. The estimates from the strain gage array have the same general shape as the results from the load cell, but have a 10-20 dB difference in the translation force estimates at many frequencies. Again, this indicates that the calibration matrix varies significantly with a large steering angle.

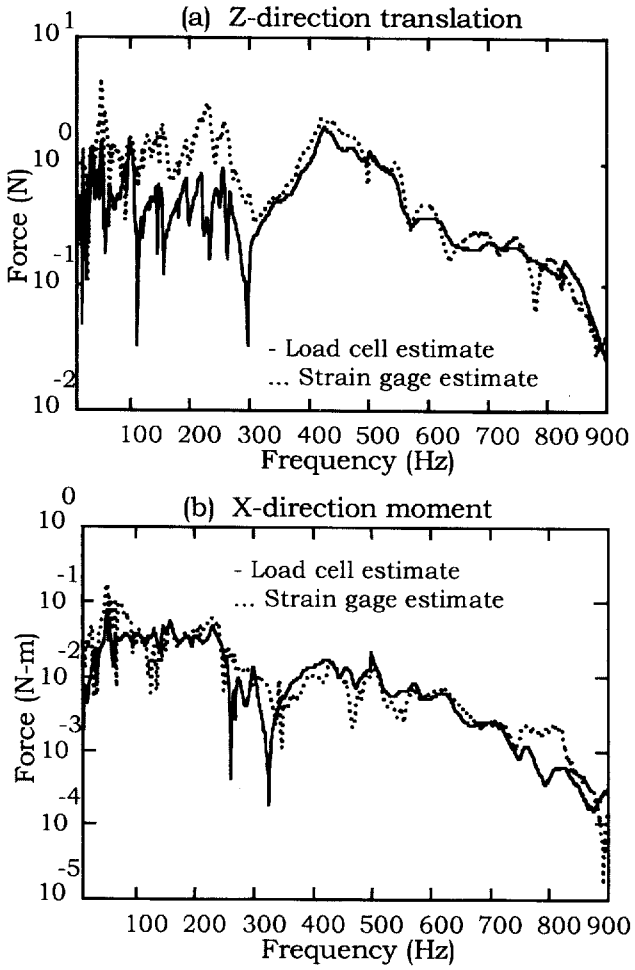

Figure 16: *Sample operating force estimates using baseline calibration matrix and steering angle 25° to left operating data*

6. NEGLECTING THE EFFECTS OF MOMENTS

In transfer path analysis, the moments are normally neglected because there is no accurate way to measure the moment inputs. Since the 6-DOF load cell measures both translation force inputs and moment inputs, the effects of the moments on estimated responses of the vehicle can be studied.

To determine the effects of moments, the strain gage array is calibrated to the three translation force inputs and the moment inputs are neglected in the array calibration. Since the 6-DOF load cell is very sensitive to moments, the moments are not neglected in the load cell step of the array calibration.

Ideally, accelerometers would be placed at locations of interest inside the vehicle, such as the steering wheel and seat track, and the responses estimated at those locations. However, accelerometer data was not available in this test. The operating responses of the 18 strain gages are estimated using the translation calibration matrix, and compared with the measured strain gage responses.

Figure 17 shows typical strain gage operating responses in all 3 directions with the estimated responses neglecting moments.

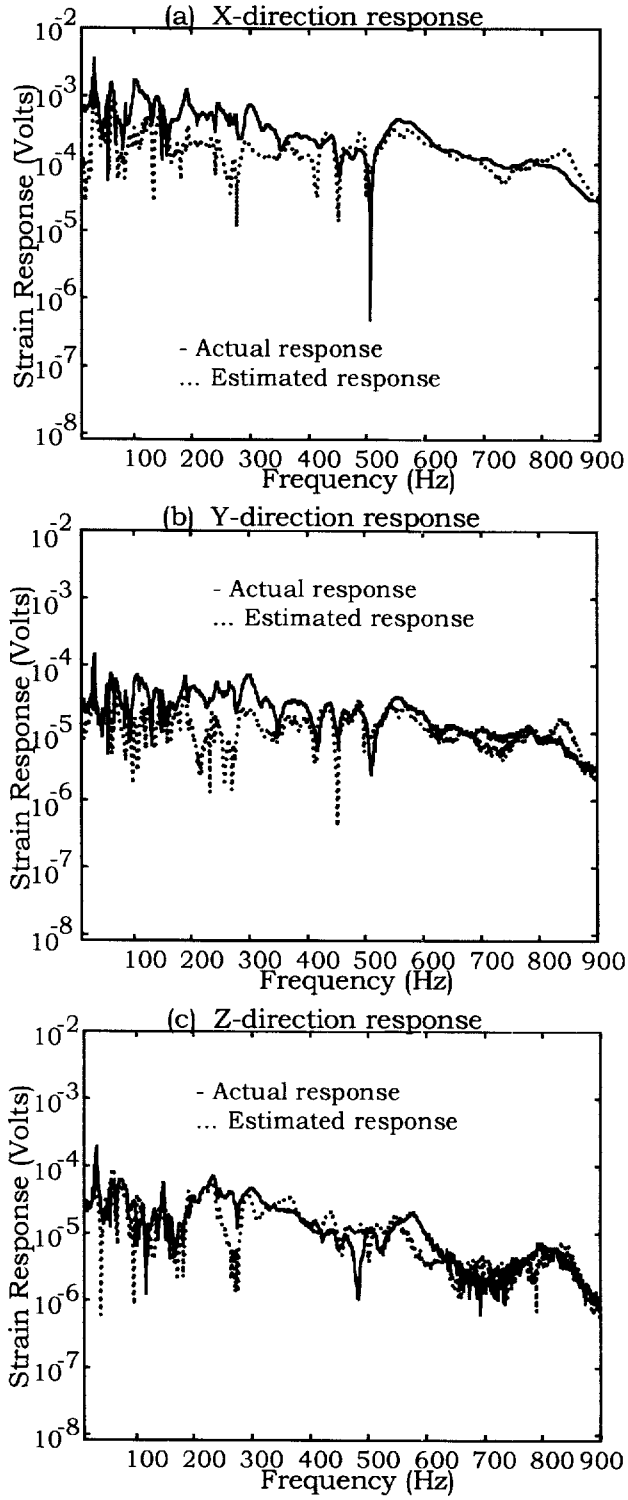

Figure 17: *Actual operating strain gage responses, and estimate responses neglecting moments.*

It is clear from figure 17 that the strain gages are sensitive to the operating moment inputs. However, no conclusions can be drawn as to the sensitivity of interior vehicle accelerations to moment inputs.

7. CONCLUSIONS

A method for estimating the three translation forces and three moments entering a steering knuckle from the wheel assembly, without modifying the steering knuckle, has been evaluated. The method involves calibrating an array of ICP strain gages placed on the steering knuckle, preferably in areas of high strain, to yield the 6 inputs. The strain gage array is calibrated using a 6-DOF load cell and the inverse FRF method. The 6-DOF load cell is calibrated separately using a rigid body calibration mass having known inertia properties. Perimeter reference accelerometers are used to measure the motion of the calibration mass, and F=ma is used to estimate the resulting three translation force inputs and three moment inputs to the load cell.

Laboratory operating data was acquired by attaching the load cell and impact mass to the instrumented steering knuckle on the vehicle, and impacting on the impact mass. This allowed for a verification check on the method with input estimates from the strain gage array and from the load cell. Because the strain gage array is calibrated to the forces entering through the wheel only, any changes to the steering knuckle boundary conditions will affect the array calibration matrix. To investigate this, operating data was taken with the vehicle in a baseline configuration of level height and 0° steering angle, 5" above level height and 0° steering angle, and level height with 25° steering angles to the right and left. The array calibration matrix from the baseline configuration was used to process all operating data. The results indicated that the calibration matrix does not vary significantly with vehicle suspension height, but does vary significantly with large steering angles. Therefore, the method is currently valid for chassis dynamometer testing and road testing without large steering angles. The effects of small steering angles on the array calibration matrix will be evaluated in future testing.

To study the effects of moment inputs, operating strain gage responses were reconstructed using an array calibration matrix that neglected moment inputs. The reconstructed responses were compared with the measured responses. The results indicated that the strain gage responses are sensitive to moments. The effects of moments on reconstruction of steering wheel and seat track operating accelerations will be investigated in the near future.

When the vehicle was suspended for the array calibration measurements, the dynamics of the struts were different than actual operating dynamics of the struts. A possible alternative array calibration test method is to place the vehicle on a 4-poster and apply forces and moments through the 4-poster exciter.

In order to reduce the sensitivity of the array calibration to changes in steering knuckle boundary conditions, an alternative test method will be evaluated in the near future. Instead of a strain gage array, three 3-DOF load cells located at the three steering knuckle bolt locations will be used. The 9 channel 3-DOF load cell array will be calibrated to the 6 inputs in the same manner as the strain gage array, using a 6-DOF load cell.

8. ACKNOWLEDGEMENTS

The authors would like to thank Joe Juan of Ford Motor Company for the support of this project.

9. REFERENCES

[1] Dumbacher, S.M., Brown, D.L., and R. Merkel, *Noise Path Analysis Test Methods*, Proc. of the 23rd International Seminar on Modal Analysis, Leuven, Belgium, September 1998.

[2] Dumbacher, S.M., Brown, D.L., and R. Merkel, *New Sensors for Noise Path Analysis Testing*, Proc. of Internoise 98, Christchurch, New Zealand, November 1998.

[3] Stebbins, M.A., *Calibration and Application of Multi-Axis Load Cells*, Masters Thesis, 1997, University of Cincinnati.

[4] Stebbins, M.A and D.L. Brown, *Rigid Body Intertia Property Estimation Using a Six-axis Load Cell*, Proc. of the 16th International Modal Analysis Conference, Santa Barbara, CA, 1998.

[5] Witter, M.C., Brown, D.L., and R.W. Bono, *Broadband 6 DOF Accelerometer Calibration Via Impact Excitation*, Proc. of the 16th International Modal Analysis Conference, Santa Barbara, CA, 1998.

[6] Witter, M.C., Blough, J.R., and D.L. Brown, *Measuring the 6 Degree of Freedom Driving Point Frequency Response Function Using a 6 DOF Impedance Head and its Validation*, Proc. of the 23rd International Seminar on Modal Analysis, Leuven, Belgium, September 1998.